

# EVLA Memo 90

## Performance Tests of the EVLA C-Band Feed

Rick Perley and Bob Hayward  
NRAO

February 16, 2005

### Abstract

Results of tests on the performance of the EVLA C-Band feed design are presented. The efficiency rises from 0.55 at 4 to 5 GHz to 0.65 from 6 to 8 GHz. The cold-sky system temperature, at zenith, is 23.5K. The contribution to system temperature from ground spillover is constant between the zenith and an elevation of 30 degrees, increases by about 1K to 20 degrees elevation, then more quickly at lower elevation, reaching 10 to 15 K at the limiting elevation of 8 degrees. The spillover contribution is higher at the lower end of the 4 – 8 GHz band. The beamwidth at 4.85 GHz is circular to 1%, and the first sidelobes in the plane of the quadrupod legs are down by 14 dB from the maximum.

Compared to the existing feed, the EVLA feed has slightly lower efficiency (at 4.85 GHz), slightly lower sidelobe structure, and higher spillover at elevations below 20 degrees. The EVLA feed/receiver has vastly better sensitivity and wider frequency coverage than the current feed/receiver.

## 1 Introduction

A primary requirement for the EVLA is to provide complete frequency coverage from 1 to 50 GHz with the highest possible sensitivity. This requirement will be met by installation of eight high-performance wide-bandwidth receivers and feeds located around the Cassegrain feed ring, one of which is the 4 – 8 GHz feed (C-Band). Two prototype wide-band horns designed by S. Srikanth are now mounted on the EVLA test antennas and are available for performance testing.

We report here on the results of performance tests on the feed mounted in EVLA antenna #13. The parameters measured were: the cold-sky system temperature, the illumination spillover, the antenna efficiency, the location of the phase center, and the antenna power pattern, including the nearby sidelobes. Most of these parameters were determined at five frequencies spanning the entire design range of the feed. For comparison, tests of a VLA antenna at a single frequency were also made.

## 2 Test Setup

The goal of these measurements was to ascertain the performance of the antenna/feed/receiver combination. It is thus advantageous to make the total-power observations of the power provided by the receiver at its output, rather than at the end of the signal transmission chain, as the latter could include performance losses associated with the various conversions employed. We thus utilized the same total power measurement system utilized for the L-Band tests, as described in EVLA Memo #85.

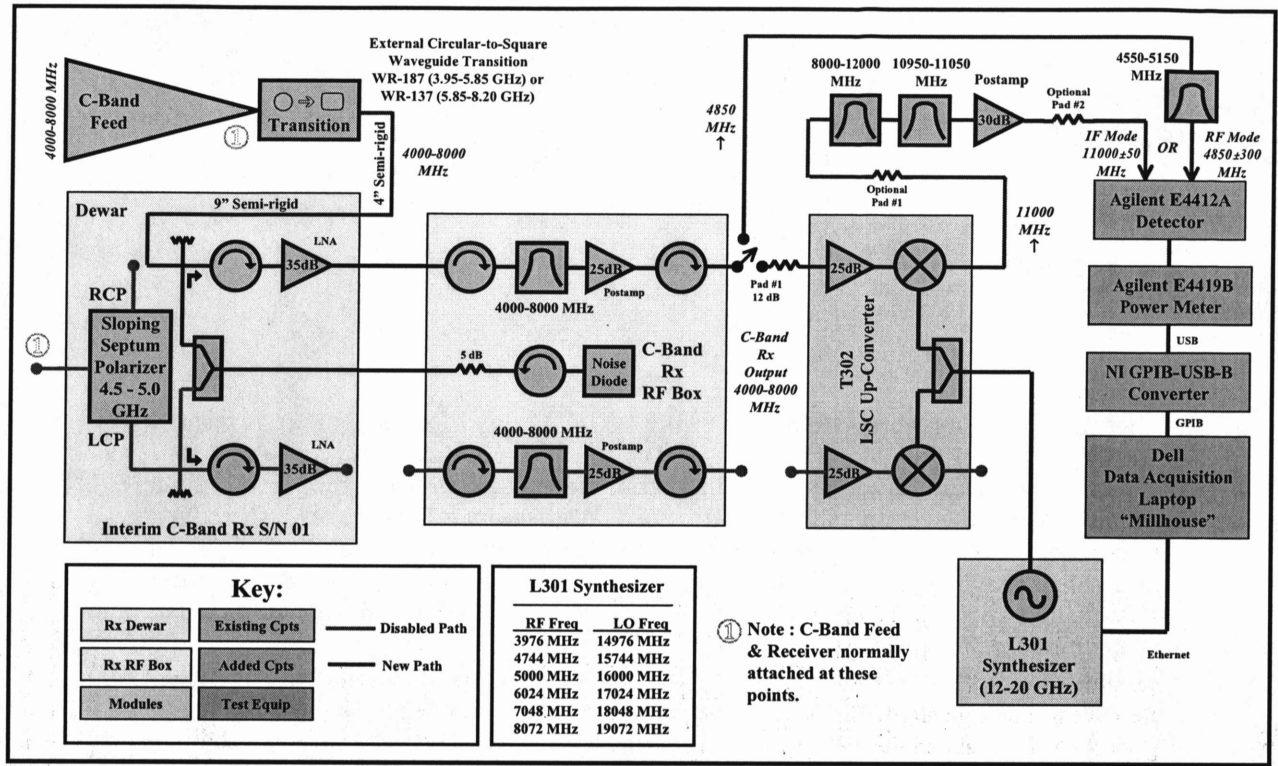


Figure 1: The setup used for determining the performance of the new C-Band feed. The orange rectangle in the upper left indicates the external circular-to-square waveguide transitions used to couple the horn to the receiver, via a short length of semi-rigid cable. With this setup, total-power measurements by the Agilent detector and power meter (purple boxes on the right side) could be made either at the RF output (top path in the upper right), or at the output of the LSC (T302) converter (pink rectangle on the right side).

A key goal of these tests was to measure the performance over the entire frequency range of 4 – 8 GHz. As the wide-band ortho-mode transducer (OMT) for this band is not yet available, we employed two specially designed circular-to-rectangular waveguide transition devices to couple the feed output to the cooled receiver. The two transition units are designed to cover 3.95 – 5.85 GHz, and 5.85 – 8.2 GHz, respectively. The single (linearly polarized) output of these transition units was connected to the input of the cooled receiver through a short (10 cm) piece of semi-rigid coax. An additional 23 cm piece of semi-rigid coax was added internally to convey the signal to the cold amplifier. This arrangement, although permitting tests throughout the entire frequency range, considerably degraded the sensitivity, as the short cable, being at room temperature, and the longer internal cable, at a median temperature of perhaps 150 K, contributed approximately 50 K to the system temperature. The arrangement described above was utilized for the tests taken in late 2004. In February 2005, a narrowband VLBA-style cooled sloping septum polarizer was attached to the C-band horn, permitting us to make single-frequency observations with the sensitivity expected from the final wide-band OMT/receiver combination.

## 2.1 Calibration

We utilized the same calibration methodology described in EVLA Memo #85, using hot and cold loads to calibrate the system gain and receiver temperature. The hot load consisted of two vertically-stacked two foot square pieces of absorber, sufficient to completely cover the aperture of the horn. The temperature of the absorber was measured by a thermometer inserted into the middle of the bottom piece. The cold load was simply the cold sky, whose total temperature is known to probably an accuracy of 5K due to the uncertain contribution from scattering of ground radiation. A discussion of the effects of this uncertainty is at the end of this section.

The system linearity was checked by measurement of the power contributed by the internal noise power diode. The zero-offset of the system was regularly removed through internal calibration of the power meter. Presuming linearity and zero offset, the relationship between the measured output power  $P$  and the input power as characterized by the temperature  $T$  is simply:

$$P = GT \tag{1}$$

where  $G$  is the conversion constant.

The conversion constant is then found to be

$$G = \frac{P_h - P_c}{T_h - T_c} \tag{2}$$

where the subscripts  $h$  and  $c$  denote the measured hot and cold powers and the (reasonably well known) input temperatures.

The hot load temperature can be written as the sum of contributions from the absorber, receiver, and stray emissions:  $T_h = T_{abs} + T_r + T_{st}$ , where the last term accounts for any contribution due to the horn itself and leakage of outside power through the horn. Similarly, the cold load power can be written as the sum of contributions from the receiver, the atmosphere, the cosmic black-body radiation, ground spillover, and a stray contribution:  $T_c = T_r + T_{atm} + T_{bb} + T_{sp} + T_{st}$ . The receiver temperature and stray temperature are both constants and hence cannot be distinguished in our tests, so we define their sum to be  $T_R$ , which can then be determined from a pair of hot and cold observations:

$$T_R = \frac{T_h P_c - T_c P_h}{P_h - P_c} \tag{3}$$

where  $T_c$  is the actual cold sky temperature (the sum of the 2.74 K CMB, 1.5 K atmospheric emission, and spillover), and  $T_h$  is the equivalent thermodynamic temperature of the hot load.

All of the contributions listed above are well known except for the spillover, which must be provided by calculation, or otherwise assumed. For these tests, we have assumed the cold sky temperature is 10 K above the receiver temperature, so the spillover contribution is 5.75 K at the zenith. We believe it most unlikely that this quantity is in error by more than 5 K.

An error in the spillover temperature reflects almost linearly into an error in the receiver temperature:

$$\delta T_R = -\delta T_{sp} \frac{P_h}{P_h - P_c} \approx -\delta T_{sp} \tag{4}$$

since  $P_h \gg P_c$ , so that an error of +5 degrees in the assumption of the spillover temperature translates into an underestimate of the receiver temperature by that same amount.

An error in the spillover temperature also affects the determination of the antenna efficiency, since the efficiency is determined by the increase in antenna temperature due to the power from a source of known spectral flux density and the estimation of this increase depends on the calibration. It is straightforward to show that the fractional error in the derived efficiency,  $\delta\epsilon/\epsilon$  is given by

$$\frac{\delta\epsilon}{\epsilon} = \frac{-\delta T_{sp}}{T_h - T_c} \approx \frac{-\delta T_{sp}}{T_h} \tag{5}$$

so that, for example, if our value of the cold sky temperature due to the uncertain contribution from ground spillover is incorrect by 5K (and it can be no larger than this), than the error in the derived value of efficiency is  $\sim 5/300 \times \epsilon \approx 1\%$ , a negligible error.

In this analysis, it has been assumed that the input power comes entirely from the main beam – that is, the main beam efficiency is 100%, whereas in fact this is closer to 75%. The effect of this assumption will be an error in the assumed values of the contributions from the cosmic background and atmospheric radiation. However, these errors will be very small, as the quantities concerned are small (2.74 K and 1.5 K sec  $z$ , respectively), and as the forward efficiency (the fraction of input power originating within  $\sim 8$  degrees of the main beam) is close to 90%, so that the atmospheric emission can be characterized by its value at the beam center elevation.

### 3 The Quantities Determined

Observations of the system temperature, focus gain curve, and system efficiency were made at 3976, 5000, 6024, 7048 and 8072 MHz at the output of the LSC converter, all with 100 MHz bandwidth at the IF frequency of 11 GHz. In addition, we took measurements of these quantities, plus the antenna primary beamshape and sidelobes, at 4850 MHz with 600 MHz bandwidth at the output of the receiver itself, for comparison with the IF quantities. The methods for determining each of the required characteristics are summarized below. For comparison, observations of these same quantities were made with VLA antenna #6, at a frequency of 4866 MHz.

#### 3.1 Focus Curve

The subreflector's location for maximum forward gain, and the focus loss curve, were determined at all frequencies by moving the subreflector over its range of motion while observing the strong radio source Cygnus A.

#### 3.2 Illumination Spillover and Scattering

To measure the spillover, the antenna was driven manually from 90 degrees elevation to 8 degrees, and the total power recorded.

#### 3.3 Cold Sky System Temperature

This crucial sensitivity parameter was determined by high-elevation observations of the cold sky, taken during the tipping observations described above. Because of the 'hybrid receiver' setup utilized to obtain the other quantities over the full frequency range, we could not determine the expected EVLA C-band system temperature over the frequency range. We utilized the cooled VLBA OMT to determine the expected system temperature at a single frequency, 4850 MHz.

#### 3.4 Antenna Efficiency

The efficiency of the feed/antenna combination was measured through observations of the increment in power due to a source of known flux density. We used both Cygnus A and the standard flux density calibrator 3C295.

#### 3.5 Antenna Beamwidth and Sidelobes

Radial scans through Cygnus A, extending about 0.8 degrees on each side of the beam maximum, were made to measure the size and shape of the main response lobe, and the inner two sidelobes. Cuts at four different position angles were made at 4850 and 6024 MHz.

## 4 Results

### 4.1 Focus Location

Focus curves were measured at six frequencies, with the results shown in Fig. 2. As expected, there is a small,  $\sim 1.5$  cm shift in optimum subreflector position across the band. An unexpected result was that the optimum position is not a monotonic function of frequency, but rather reaches a minimum near mid-band, then slowly rises towards the upper frequency end. The beneficial result of this is that a single subreflector position near 3 cm offset will enable wide-band continuum observations with no more than 10% defocussing loss at the low-frequency end of the band, and less than 1% at 6 GHz.

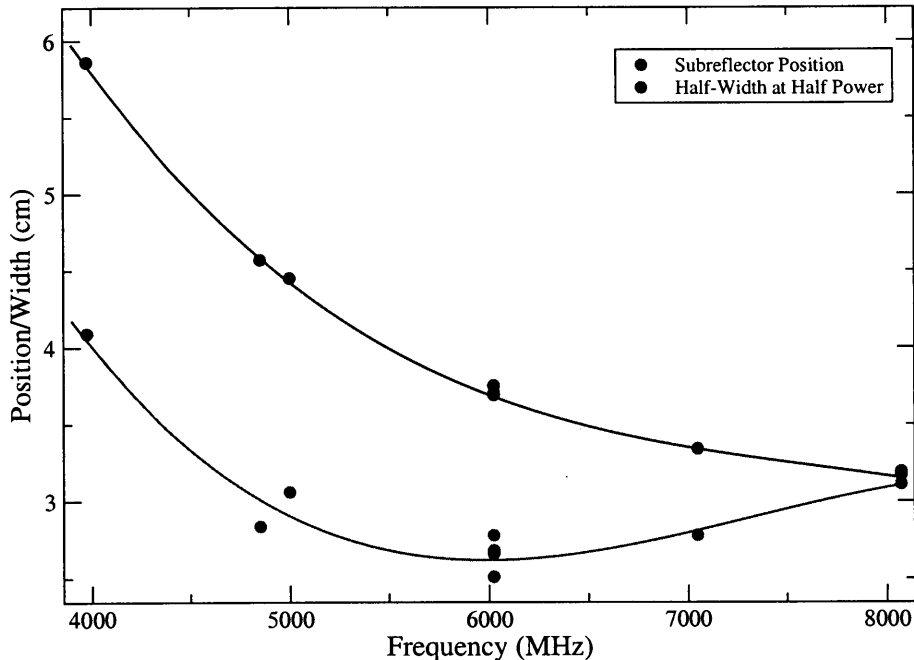


Figure 2: The optimum position of the subreflector for six frequencies (red dots), and a best fit (red line). The blue dots show the subreflector offset, relative to the best fit position, at which the forward gain is reduced by half. The reference position is at 16000 octal counts.

### 4.2 Cold Sky System Temperature

The measurements of the cold sky system temperature were taken from the minimum value of system temperature determined from the sky dips used to determine the variation of spillover with elevation. As noted in Section 2, we had to use a receiver system which is not representative of the final EVLA in order to assess the feed performance over the full frequency range. These measurements are thus not useful in characterizing the expected system temperature.

To get a fair measure of the anticipated final system sensitivity, a cooled VLBA polarizer was installed in early February 2005. The sky dip obtained from this system (at 4850 MHz) is shown in Fig 3.

The total (zenith) system temperature was found to be slightly in excess of 23K – a very satisfactory value! Subtracting the known atmospheric contribution of 1.5 K, and a CMB contribution of 2.75 K, the sum of the receiver and ground spillover contributions is then 19 K, which when compared to the bench measurement of the receiver temperature of 18 K suggests a zenith spillover contribution of only 1 K. However, it is believed more likely that the bench receiver temperature

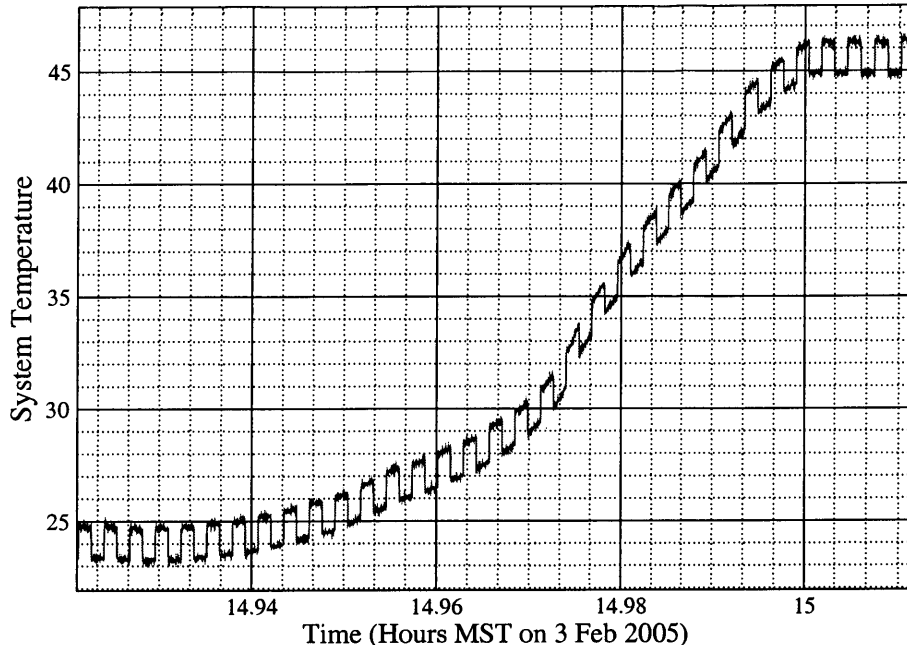


Figure 3: A sky dip at 4850 MHz, taken with the cooled VLBA polarizer on the EVLA test antenna. This setup is expected to be a good predictor of the final EVLA system temperature performance. The total system temperature at high zenith angle is about 23 K. The square wave seen in the trace is the 1.42 K noise diode calibration, applied with a 10 second period.

is too high by a few degrees because the contribution of a short cable on the cold load  $50 \Omega$  termination utilized in the lab measurements has not been accounted for. If this contribution is about 4 K, then the receiver temperature is 14 K, and the zenith spillover is 5 K.

The 23 K system temperature is to be compared to the 58 K system temperature measured on VLA antenna 6. The major portion of the difference is due to the use of an uncooled polarizer for the VLA. For the EVLA, the polarizer will be located in the cryostat.

### 4.3 Illumination Spillover

Sky dips were made at all frequencies in order to determine the variation with elevation of the total system temperature. To separate the contribution from spillover from those due to atmospheric emission and cosmic background, the 2.74 K CMB (assumed constant with elevation), and an estimate of the atmospheric emission equal to  $1.5 \sec(z)$  K were subtracted. The remainder then reflects the sum of the unchanging receiver temperature  $T_R$  and the ground spillover. For all frequencies, this remainder is a minimum near an elevation of 60 degrees. The value at 60 degrees elevation was then subtracted to give the variation of the ground spillover contribution with elevation. Note that the spillover contribution at 60 degrees elevation is unknown, and cannot be separated from the receiver temperature from these data. The only constraint we have on spillover comes from comparing the total system temperature with bench measurements of the receiver temperature, and accounting for the atmospheric, CMB, and stray contributions, as described in the preceding section.

The results of this analysis are shown in Fig. 4. It should be noted that the ground spillover contribution to the EVLA feed is greatest at the low end of the band – reaching 15 K (over the high-elevation value) at the limiting elevation of 8 degrees. At the high end of the band, the excess is notably less – about 11 K at the lowest elevations – but still considerably more than the VLA feed’s excess contribution of only 6 K at this elevation.

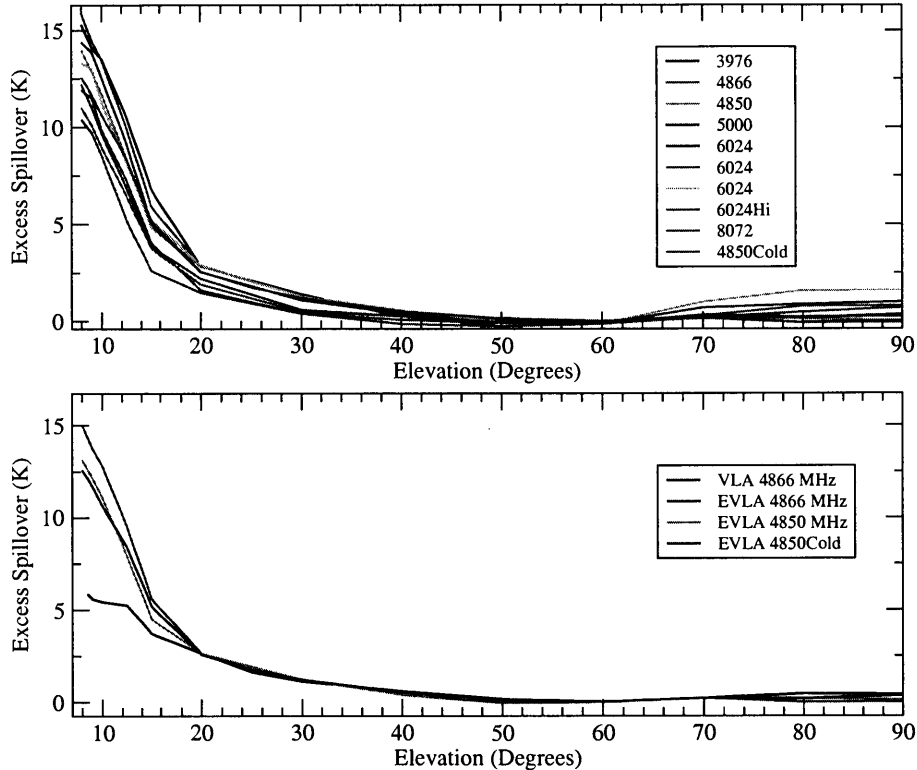


Figure 4: Upper Panel: The excess spillover for all frequencies. The system temperature at 60 degrees elevation defines the reference value. The highest values for spillover are at the lower end of the band. Lower Panel: Comparing the spillover of the EVLA to that of the VLA (black). The spillover from the existing VLA feed is considerably less than that from the new EVLA feed at elevations below 20 degrees.

#### 4.4 Antenna Efficiency

The antenna efficiency is defined as the ratio between the actual power received by an antenna to that which traverses through an aperture of equal cross-section. In terms of the physical cross-section area,  $A_p$ , and the effective area  $A_e$ , we have

$$\epsilon = \frac{A_e}{A_p} \quad (6)$$

Observation of a point object of known spectral flux density  $S_0$  will result in an increase in antenna temperature by an amount

$$T_a = \frac{S_0 A_e}{2k} \quad (7)$$

where  $k$  is Boltzmann's constant.

With the antenna temperature in Kelvin, and the source flux density in Jy, the efficiency of a 25-meter antenna can be expressed as

$$\epsilon = 5.62 \frac{T_a}{S_{Jy}} \quad (8)$$

The efficiencies were determined by on-off observations of the well known calibrator Cygnus A. With a source angular size of two arcminutes, and an antenna FWHM beam size of 10.9 to 5.3 arcminutes (from 3976 to 8072 MHz), a modest correction for resolution is necessary.

Good pointing is also required for an accurate determination of the efficiency. Because accurate pointing coefficients for the test antenna have not yet been determined, a four-point offset pattern was utilized to determine the pointing error. Presuming the forward gain follows a gaussian form:

$$P = P_0 \exp \left[ -\ln 2 \left( \frac{r - r_0}{r_{1/2}} \right)^2 \right] \quad (9)$$

the offset  $x_0$  in each plane can be determined from power observed at the two offset observations,  $P^+$  and  $P^-$  to be

$$x_0 = \frac{r_{1/2}^2}{4 \ln 2 \Delta} \ln \left( \frac{P^+}{P^-} \right) \quad (10)$$

where  $\Delta$  is the offset angle, and  $r_{1/2}$  is the half width to half power. The assume gaussian form is sufficiently accurate within the half-power for these corrections, but increasing levels of doubt should accompany corrections made when the offset plus pointing error is significantly larger than the half-width angle.

All the data taken on Cygnus A are given in Table 1.

EVLA Antenna C-Band Efficiency Measurements											
Freq MHz	Date	Trans	Tsys K	Tcal K	r	Corr	Tcyg K	Tcyg K	Scyg Jy	$\epsilon_r$	$\epsilon_c$
3976	3 Nov 04	Lo	68	10.3	2.3	1.13	42.9	48.6	495	.49	.55
4850	19 Nov 04	Hi	78	13.5	0.4	1.01	32.7	32.9	389	.49	.50
4850	3 Feb 05	VLBA	23	1.42	0.8	1.02	37.6	38.4	389	.54	.55
5000	19 Nov 04	Hi	71	13.2	0.0	1.00	35.9	35.9	375	.54	.54
6024	11 Nov 04	Lo	80	13.5	1.1	1.07	27.5	39.5	297	.52	.56
6024	12 Nov 04	Lo	83	14.0	1.5	1.10	31.3	34.5	297	.60	.65
6024	12 Nov 04	Hi	81	13.6	1.6	1.15	30.7	35.2	297	.58	.67
6024	19 Nov 04	Hi	80	13.5	1.1	1.07	32.5	34.5	297	.59	.65
7048	19 Nov 04	Hi	78	10.8	1.1	1.11	24.0	26.6	243	.56	.62
8096	19 Nov 04	Hi	87	11.7	1.2	1.15	20.2	23.1	204	.55	.64

Table 1: The EVLA C-Band efficiency measurements. The columns are: (1) Frequency in MHz; (2) The date of the observation; (3) The transition used between the horn and the amplifier; (4) The derived system temperature; (5) The derived calibration noise diode temperature; (6) The radial pointing error in arcminutes; (7) The correction for pointing error and resolution; (8) The observed antenna temperature for Cygnus A, corrected for focus, but not for resolution and pointing; (9) The corrected antenna temperature; (10) the flux density of Cygnus A in Jy; (11), The derived efficiency without correction for focus and pointing; (12) The derived efficiency with all corrections applied. Note that the low efficiency for 4850 MHz on 19 Nov is due to the hi-frequency transition used for this low frequency observation, and that the observation at 6024 on 19 Nov was made without a pointing offset determination, and the offset shown is that for 7048 MHz, made shortly afterwards.

A single observation of the small-diameter calibrator 3C295 was also made at 4850 MHz on 3 Feb 2005. The efficiency derived was 0.57, in excellent agreement with the value derived from Cygnus A taken the same day.

Observations of Cygnus A were also made with VLA antenna 6 using the same measurement system on Nov 24. The efficiency derived was 0.61 at 4850 MHz.

#### 4.5 Antenna Beam and Sidelobes

The final measures made were of the antenna primary beamshape and the inner sidelobes. Ideally, we would have liked to have used the holographic raster scanning modes for this. However, the

software to drive the EVLA antenna in this grid pattern is not yet available, so we utilized simple cross-cuts at various azimuths.

The results for the EVLA at 4850 MHz are shown in Fig. 5.

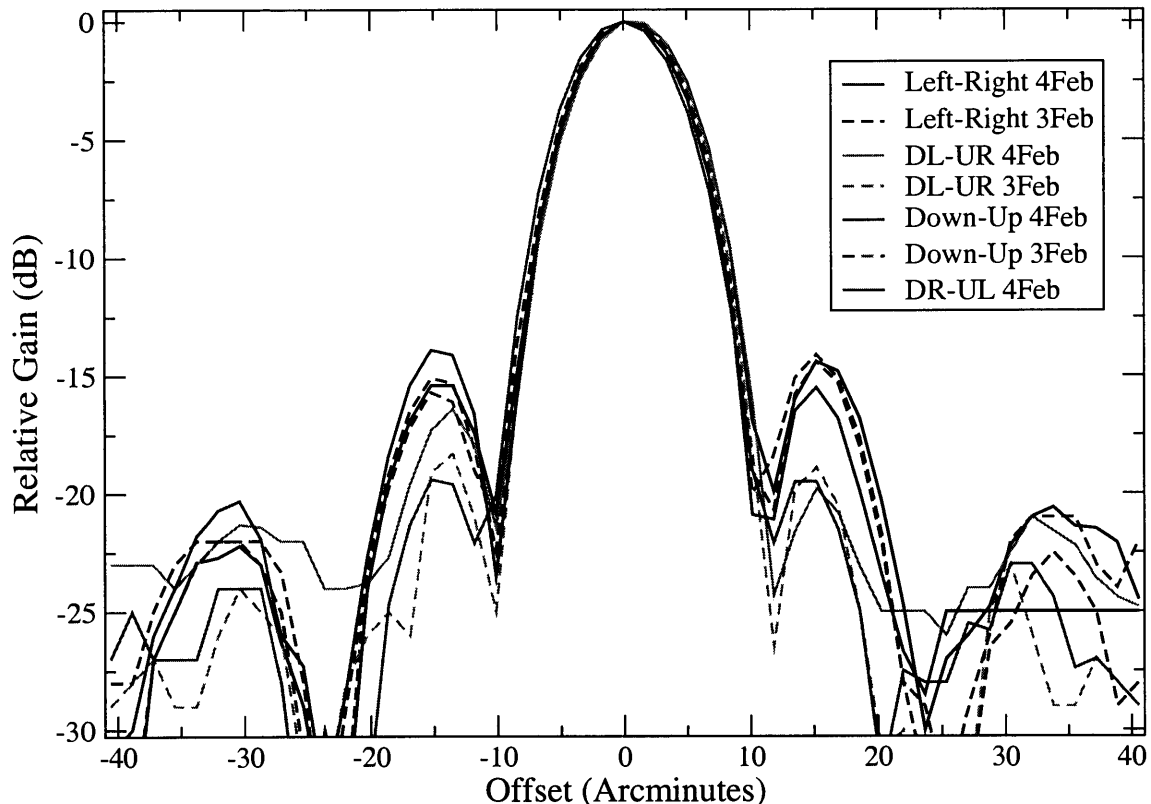


Figure 5: Four cuts through the EVLA Antenna 13 at 4850 MHz. The sidelobe levels are higher in the horizontal and vertical cuts because of the quadrupod legs.

Fitting simple quadratic fits to the central portion of these cuts gives the half-width to half-power as 8.94 arcminutes, with a variation (amongst all cuts) of about 0.05 arcminutes – well within the measurement error. This half-width is marginally larger (about 3 arcseconds) than the VLA’s beam at the same frequency.

These are to be compared to the beam shape from the 4850 MHz observations of Cygnus A with VLA antenna 6. The cross-cuts are shown in Fig. 6. The half-widths measured from these VLA data are 8.86 arcminutes – identical to the interferometer measurements averaged over all antennas, and slightly less than that measured for the EVLA test antenna. Similarly, note that the height of the first sidelobes, especially in the principal planes, is slightly less for the EVLA test antenna than the VLA antenna, indicating a slightly softer illumination. Such a softer illumination will also reduce efficiency, zenith spillover, and system temperature.

Cuts through the EVLA antenna beam were also made at 6024 MHz. These are shown in Fig. 7. In this case, the cuts were made continuously, so we have no reference point with which to determine the offset in pointing. Hence, only the sidelobe levels can be determined from these observations.

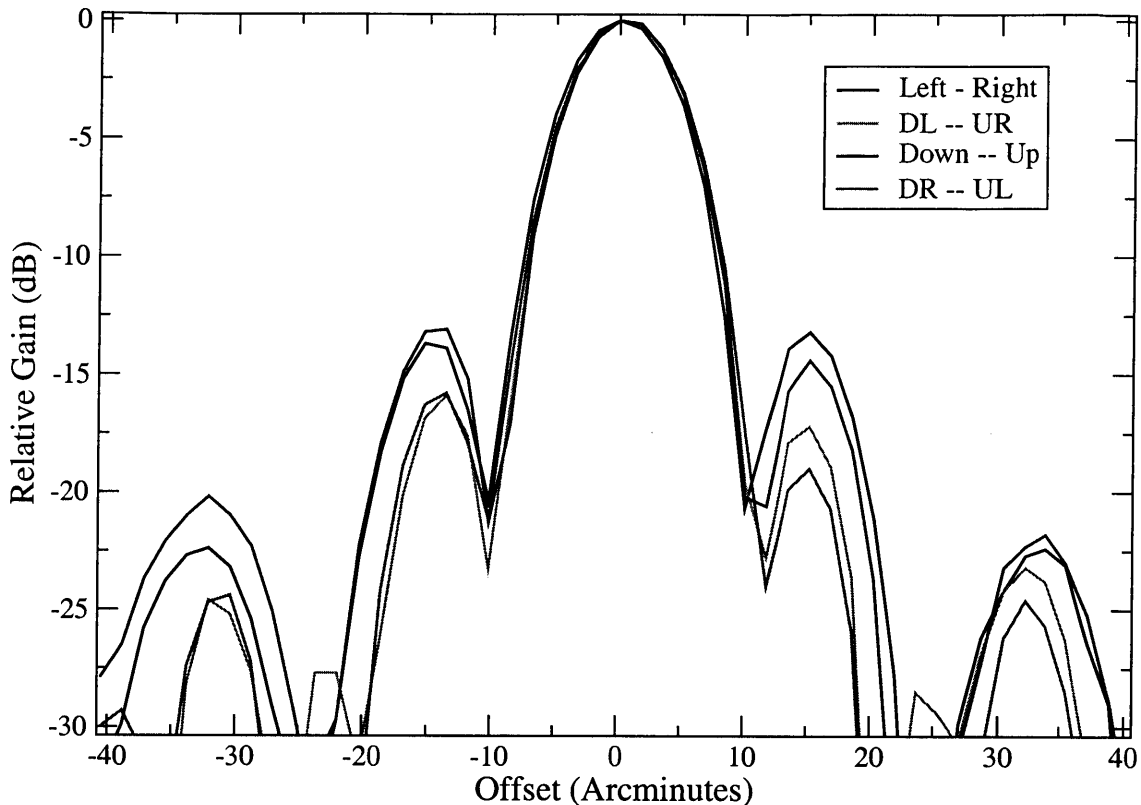


Figure 6: Four cuts through the VLA Antenna 6 at 4850 MHz. The sidelobe levels are higher in the horizontal and vertical cuts because of the quadrupod legs.

## 5 Discussion

We define our figure of merit as

$$M = \frac{1000\epsilon}{T_{sys}} \quad (11)$$

From our observations for VLA antenna #6,  $M = 10.52$  at 4850 MHz, while for the test EVLA antenna,  $M = 23.8$  – more than twice as good at the same frequency. Furthermore, the EVLA feed is extremely broad-band (with excellent performance over a frequency range of at least 3950 to 8100 MHz), while the VLA feed is limited to the narrow range 4500 – 5000 MHz. The principal reasons for the sensitivity improvement is the removal of the room-temperature polarizer and its associated waveguide, plus an improved wide-band receiver. The mean efficiency of the new feed is the same as the old – about 60%. The single negative factor for the new design is its increased spillover. However, the increment is small – no more than 8 K over the VLA feed – and is only appreciable at very low elevations – below 15 degrees.

In terms of the System Equivalent Flux Density,

$$SEFD = 5620/M \quad (12)$$

we find, with  $M = 23.8$ ,  $SEFD = 236$  Jy – about 10% better (i.e., less) than the requirement for this band given in the EVLA project book.

The conclusion is clear – the new EVLA feed and receiver meets the project requirements, and is a great improvement over the existing system.

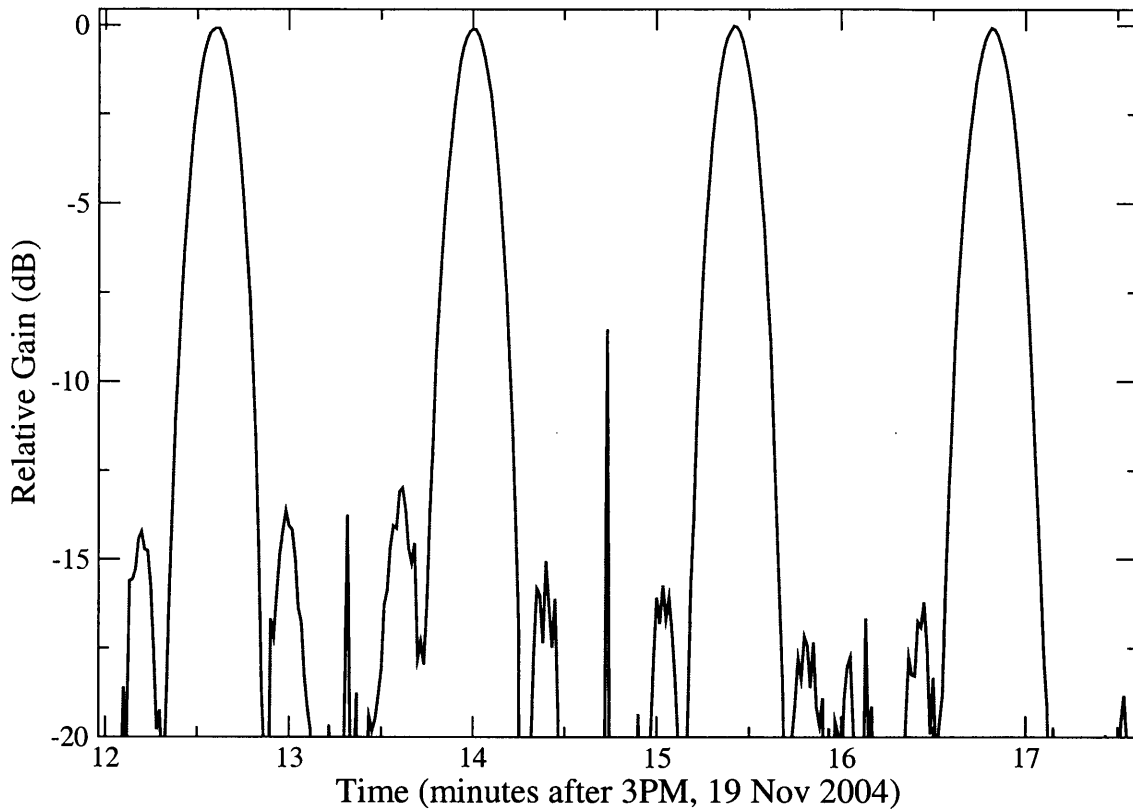


Figure 7: Four cuts through the EVLA Antenna 13 at 6024 MHz. The left-side pair are in the planes of the quadrupod legs, the right-hand pair are at plus and minus 45 degrees. The first sidelobes in the plane of the support legs are down about 13 to 14 dB, in agreement with the cuts at 4850 MHz. There is a significant asymmetry in the height of the sidelobes in the second cut, likely due to small misalignment of the feed.

## 6 Acknowledgements

We thank Barry Clark and Ken Sowinski for their patient assistance in responding to our many requests to drive the test antenna in various peculiar ways. We thank Hollis Dinwiddie for improvements to the data acquisition software which significantly improved the test sensitivity.